A Robust Initialization Scheme for a Lateral Trajectory Optimization Problem with Time of Arrival Windows

Abraham K. Ishihara

Carnegie Mellon SV, NASA Ames Research Center, Moffett Field, CA.

Nhan Nguyen

NASA Ames Research Center, Moffett Field, CA

Yi Luo

Carnegie Mellon University, Department of Mechanical Engineering, Pittsburgh, PA.

Jose Benavides

Mission Critical Technologies, NASA Ames Research Center, Moffett Field, CA 94035

John Kaneshige

NASA Ames Research Center, Moffett Field, CA

We present a robust initialization scheme that estimates parameter values for the numerical solution of a two-point boundary value problem. The two-point boundary value problem formulation stems from the optimization of a cost functional subject to the dynamics of a simplified lateral aircraft model and other constraints. Leveraging regular perturbation methods, initial parameter estimates are analytically determined and used to initialize a gradient descent optimization routine which is shown to rapidly converge over a range of initial aircraft positions and heading angles. Additionally, the velocity of the aircraft is optimized to ensure the trajectory of the aircraft terminates within a desired region in both time and space.

Key words: ***Optimal Lateral Trajectory Generation***

I. Introduction

Over the next several decades, it is predicted that the number of commercial aircraft in operation will increase rapidly posing significant challenges for the current air traffic management system [6]. Next generation air traffic management system concepts [9, 11] (termed NextGen) have been proposed to accommodate this increase in air traffic while simultaneously guaranteeing safety, addressing environmental concerns, and avoiding congestion and delays. The system may include substantial improvements in automation resulting in a significant reduction in the manual work-load currently imposed upon human air-traffic controllers. Human air-traffic controllers are envisioned to remain an integral part of the system, however, automation will enhance the ability of air-traffic controllers to focus their attention more on critical tasks and less on tasks that can be accomplished by intelligent algorithms and code. For example, currently, aircraft follow fixed paths between destinations utilizing a set of path primitives. However, these paths may not be optimal for a number of reasons including congestion, delays, off-nominal operation, weather conditions, and fuel and environmental constraints. Algorithms that rapidly compute optimal trajectories in real-time would be beneficial.

It has been envisioned that NextGen will extend the current concept of an aircraft trajectory to four dimensions or 4D (three spatial, one temporal) and may include multiple Required Time of Arrival (RTA) constraints at waypoints along the entire path [3]. This extension has been termed Trajectory Based Operations (TBO) and represents a paradigm shift to a more strategic approach in which individual aircraft trajectories are planned, generated, and executed in 4D. This will enhance the predictability of aircraft locations throughout the flight phases, enabling more efficient use of the airspace and, ultimately, increasing overall capacity. TBO also includes the concept of Controlled Time of Arrival (CTA) windows [11] in which there exist requirements at a number of waypoints specifying the minimum and maximum time of arrival. It is envisioned that CTAs may change over time due to a number of factors

including traffic congestion, weather, and inability to follow a given reference trajectory precisely. In the case of the latter, a new trajectory may be required and a corresponding *feasible* CTA window if the previous one is deemed *infeasible*. The new trajectory, termed guidance trajectory, may need to be continually updated based on current aircraft position data. The guidance trajectory may be displayed to the pilot in order to guide the aircraft from its off-nominal position back to the reference trajectory to comply with tactical objectives and constraints.

In order to rapidly compute optimal trajectories given a CTA window and current aircraft position, this paper proposes a robust initialization scheme that estimates parameter values for the numerical solution of a two-point boundary value problem. The two-point boundary value problem formulation stems from the optimization of a cost functional subject to the dynamics of a simplified lateral aircraft model and other constraints. Leveraging perturbation methods, initial parameter estimates are analytically determined and used to initialize a gradient descent optimization routine which is shown to rapidly converge over a range of initial aircraft positions and heading angles.

The main ideas are illustrated in Fig. 1.

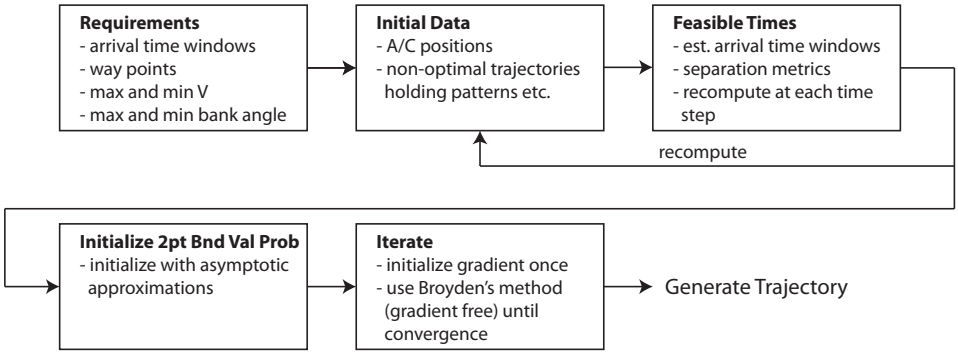

Figure 1. Block diagram depicting the main components of the algorithm.

An advantage of using this approach is that it enables a number of more complex optimization problems to be posed and solved in a reasonable amount of time. One such problem is the merging of multiple aircraft given multiple CTAs and separation assurance constraints. It is shown in simulation that separation can be optimized while satisfying multiple CTA requirements.

The remainder of this paper is organized as follows: In Section II, we present the problem formulation. In Section III, we discuss the asymptotic approximation of the solution to the optimal control problem. In Section IV, we present the computation of feasible regions in both time and space. The purpose of this computation is to enable a flight controller to choose (and change on the *fly*) a desired CTA window for one or more aircraft. In Section V, we present several examples illustrating the algorithm, including a multiple aircraft merging problem with separation assurance. We also present an example where the optimally generated trajectories are fed into an adaptive backstepping lateral control system. A damaged aircraft is simulated and is shown to exceed the separation assurance bound triggering the re-computation of all optimal trajectories. Conclusions are given in Section VI.

II. Problem Formulation

Consider the following nonlinear dynamical system

$$\dot{\vec{x}} = f(\vec{x}, u, t) \tag{1}$$

where[a] $\vec{x} : [t_0, \infty) \to \mathbb{R}^n$ denotes the state of the dynamic system and $f : \mathbb{R}^n \times \mathbb{R}^m \times [t_0, \infty) \to \mathbb{R}^n$ is a sufficiently smooth map guaranteeing the existence and uniqueness of solutions. Here, $t_0 \geq 0$ denotes the initial time and n and m denote the dimensions of the state and control input, respectively. The solution of (1) through the initial *data* $(\vec{x}_0, t_0)$ is denoted by $\vec{x}(t; \vec{x}_0, t_0, u)$ where we have explicitly shown the dependence on the control input u. We assume u is piecewise continuous satisfying

$$U_{min} \leq u(t) \leq U_{max} \tag{2}$$

[a] In the general 12-state aircraft dynamical equations, x typically denotes the position in inertial coordinates. Hence, to avoid notational confusion, we utilize the vector overbar notation to indicate an arbitrary n-dimensional state vector.

The optimal control problem [5, 8, 13] may be loosely stated as follows: Let the cost functional be defined by

$$J(u) = \phi(\vec{x}(t_f), t_f) + \int_{t_0}^{t_f} L(\vec{x}(t), u(t), t)dt \tag{3}$$

where $\phi : \mathbb{R}^n \times \mathbb{R} \to \mathbb{R}$ is the *terminal* cost and $L : \mathbb{R}^n \times \mathbb{R}^m \times \mathbb{R} \to \mathbb{R}$ is the *running* cost. We seek an optimal control and trajectory, call them u^* and x^*, respectively, that minimize (3) subject to the control being a piecewise continuous function satisfying the constraints in (2), and the trajectory being a solution of (1) through the initial (known) data $(\vec{x}_0, t_0)$ and satisfying the final state constraints

$$F(\vec{x}(t_f), t_f) = 0$$

In the case of lateral trajectory optimization we take a simplified model considered in Michelin *et al.* [16]. The states are:

$$\vec{x} \stackrel{\text{d}}{=} \begin{bmatrix} x \\ y \\ \psi \end{bmatrix}$$

where x denotes the position, y denotes the position, and ψ denotes the heading angle of the aircraft. The dynamics are given by

$$\dot{\vec{x}} = \begin{bmatrix} \dot{x} \\ \dot{y} \\ \dot{\psi} \end{bmatrix} = \begin{bmatrix} V\cos(\psi) \\ V\sin(\psi) \\ u \end{bmatrix} \tag{4}$$

We note that number of optimization algorithms for lateral trajectories (4) have been presented in the literature [4, 7, 16, 18]. However, most of them consider the minimization of fuel or minimum arrival time. These optimization costs may not be useful for CTA window applications where timing is critical for the proper sequencing of multiple aircraft. Instead, we consider the following running cost where we set $\phi = 0$ (no terminal cost)

$$L(\vec{x}, u, t) = \frac{1}{2}u^2 \tag{5}$$

and impose the following final state constraints:

$$\begin{aligned} y(t_f) &= 0 \\ \psi(t_f) &= 0 \end{aligned} \tag{6}$$

The costate equation becomes

$$\dot{\lambda} = -\frac{\partial H}{\partial \vec{x}} = \begin{bmatrix} 0 \\ 0 \\ -\lambda_1 V\sin(\psi) + \lambda_2 V\cos(\psi) \end{bmatrix}$$

This yields (using (4)):

$$\dot{\lambda}_3 = \lambda_1 \dot{y} - \lambda_2 \dot{x} \tag{7}$$

Integrating (7) we obtain

$$\lambda_3(t) = \lambda_1 y - \lambda_2 x + c$$

where c is an arbitrary constant that will be determined later[b]

Also from (7) we conclude that λ_1 and λ_2 are constants. The transversality condition yields

$$\lambda^T(t_f) v_{\vec{x}}(t_f) = \begin{bmatrix} \lambda_1(t_f) & \lambda_2(t_f) & \lambda_3(t_f) \end{bmatrix} \begin{bmatrix} v_x(t_f) \\ 0 \\ 0 \end{bmatrix}$$

Since $v_x(t_f) \neq 0$ (perturbation at the final time) we find

$$\lambda_1 = 0 \tag{8}$$

[b]This constant will later be adjusted to guarantee that the final heading angle is equal to the desired final heading angle.

Hence, using (8) in (7) we have

$$\lambda_3(t) = -\lambda_2 x + c$$

The stationarity condition yields:

$$\frac{\partial h}{\partial u} = u + \lambda_3 = 0$$

Solving for the control, we obtain

$$u(t) = \lambda_2 x(t) - c \tag{9}$$

The above holds subject to $U_{min} \leq \lambda_2 x(t) - c \leq U_{max}$. Outside of these bounds, we appeal to the Pontryagin minimum principle.

Remark 1 *It is interesting to note that optimal control law (9) for the **nonlinear** system given in (4) subject to the cost functional given in (3) is **linear** in the state*[c].

Substituting the control law (9) into (4) we obtain

$$\dot{\psi} = \lambda_2 x(t) - c$$

Differentiating both sides we obtain:

$$\ddot{\psi} = \lambda_2 \dot{x} = \lambda_2 V \cos(\psi) \tag{10}$$

III. Asymptotic Approximation of the Optimal Trajectory

We consider an asymptotic approximation to the solution of (10) with initial data $\psi(t_0) = 0$ and $\dot{\psi}(0) = f(t)$. Specifically, we consider:

$$\hat{\psi}(t;\lambda_2) = w_0(t) + \varepsilon w_1(t) + \varepsilon^2 w_2(t) + \mathrm{O}(\varepsilon^3) \tag{11}$$

where $\varepsilon = \lambda_2 V$. Note that $w_i(t)$ is independent of λ_2 for each $i = 0, 1, 2$. At this point, we do not know λ_2, V, and c.

Substitution of the candidate asymptotic approximation (11) into (10) yields:

$$\ddot{w}_0 + \varepsilon \ddot{w}_1 + \varepsilon^2 \ddot{w}_2 + \mathrm{O}(\varepsilon^3) = \varepsilon \left(\cos(w_0) - \sin(w_0) w_1 \varepsilon + \mathrm{O}(\varepsilon^3) \right) \tag{12}$$

Balancing order by order [10], we obtain

$$\begin{array}{lrcl} \mathrm{O}(1): & \ddot{w}_0 & = & 0 \\ \mathrm{O}(\varepsilon): & \ddot{w}_1 & = & \cos(w_0) \\ \mathrm{O}(\varepsilon^2): & \ddot{w}_2 & = & -w_1 \sin(w_0) \end{array} \tag{13}$$

Integrating the $\mathrm{O}(1)$ equation twice yields:

$$w_0(t) = a_1 t + a_2 \tag{14}$$

where a_1 and a_2 are arbitrary constants. Similarly, integrating the $\mathrm{O}(\varepsilon)$ equation twice yields:

$$w_1(t) = -\frac{1}{a_1^2} \cos(w_0) + a_3 t + a_4 \tag{15}$$

where a_3 and a_4 are arbitrary constants.

Before proceeding with the $\mathrm{O}(\varepsilon^2)$ equation, we present a list of integral relations that will be used throughout the remainder of this paper.

[c] Technically speaking, the control law is an affine function.

$$
\begin{aligned}
f_0 &\overset{\mathrm{d}}{=} \int \sin(w_0)dt &&= -\tfrac{1}{a_1}\cos(w_0)\\
f_1 &\overset{\mathrm{d}}{=} \int \cos(w_0)dt &&= \tfrac{1}{a_1}\sin(w_0)\\
f_2 &\overset{\mathrm{d}}{=} \int \sin(w_0)\cos(w_0)dt &&= -\tfrac{1}{2a_1}\cos^2(w_0)\\
f_3 &\overset{\mathrm{d}}{=} \int \cos^2(w_0)dt &&= \tfrac{1}{2a_1}\left(w_0+\tfrac{1}{2}\sin(2w_0)\right)\\
f_4 &\overset{\mathrm{d}}{=} \int t\cos(w_0)dt &&= \tfrac{t}{a_1}\sin(w_0)+\tfrac{1}{a_1^2}\cos(w_0)\\
f_5 &\overset{\mathrm{d}}{=} \int \sin^2(w_0)dt &&= \tfrac{1}{2a_1}\left(w_0-\tfrac{1}{2}\sin(2w_0)\right)\\
f_6 &\overset{\mathrm{d}}{=} \int t\sin(w_0)dt &&= -\tfrac{t}{a_1}\sin(w_0)+\tfrac{1}{a_1^2}\sin(w_0)\\
f_7 &\overset{\mathrm{d}}{=} \int \sin(2w_0)dt &&= -\tfrac{1}{2a_1}\cos(2w_0)\\
f_8 &\overset{\mathrm{d}}{=} \int \sin(2w_0)dt &&= -\tfrac{1}{2a_1}\cos(2w_0)\\
f_9 &\overset{\mathrm{d}}{=} \int t\sin^2(w_0)dt &&= t f_5-\tfrac{1}{2a_1}\left(\tfrac{a_1t^2}{2}+a_2t-\tfrac{1}{2}f_7\right)\\
f_{10} &\overset{\mathrm{d}}{=} \int \cos(w_0)\sin^2(w_0)dt &&= \tfrac{1}{3a_1}\sin^3(w_0)\\
f_{11} &\overset{\mathrm{d}}{=} \int \cos^3(w_0)dt &&= f_1-f_{10}\\
f_{12} &\overset{\mathrm{d}}{=} \int t\cos^2(w_0)dt &&= t f_3-\tfrac{1}{2a_1}\left(\tfrac{a_1t^2}{2}+a_2t+\tfrac{1}{2}f_7\right)\\
f_{13} &\overset{\mathrm{d}}{=} \int t^2\cos(w_0)dt &&= \tfrac{1}{a_1}\left(t^2\sin(w_0)-2f_6\right)\\
f_{14} &\overset{\mathrm{d}}{=} \int \cos^2(w_0)\sin(w_0)dt &&= -\tfrac{1}{3a_1}\cos^3(w_0)\\
f_{15} &\overset{\mathrm{d}}{=} \int \cos(w_0)\sin(2w_0)dt &&= 2f_{14}\\
f_{16} &\overset{\mathrm{d}}{=} \int t\cos(w_0)\sin(w_0)dt &&= t f_2+\tfrac{f_3}{2a_1}\\
f_{17} &\overset{\mathrm{d}}{=} \int t^2\sin(w_0)\sin(w_0)dt &&= t^2 f_0+\tfrac{2}{a_1}f_4
\end{aligned}
\tag{16}
$$

Using (16), we compute

$$
w_2(t) = -\frac{1}{8a_1^4}\sin(2w_0)+\frac{a_3}{a_1^2}t\sin(w_0)+\frac{2a_3}{a_1^3}\cos(w_0)+\frac{a_4}{a_1^2}\sin(w_0)+a_5t+a_6 \tag{17}
$$

where a_5 and a_6 are arbitrary constants.

Boundary Conditions: At the initial time, we have

$$
\psi(0) = w_0(0)+\varepsilon w_1(0)+\varepsilon^2 w_2(0)+\mathrm{O}(\varepsilon^3) = \psi_0
$$

This yields $w_0(0) = \psi(0)$; $w_1(0) = w_2(0) = 0$. Hence, using (14),(15), and (17) we get

$$
a_2 = \psi_0 \tag{18}
$$

$$
-\frac{1}{a_1^2}\cos(a_2)+a_4 = 0 \tag{19}
$$

$$
-\frac{1}{8a_1^4}\sin(2a_2)+\frac{2a_3}{a_1^3}\cos(a_2)+\frac{a_4}{a_1^2}\sin(a_2)+a_6 = 0 \tag{20}
$$

At the final time, we have

$$
\psi(t_f) = w_0(t_f)+\varepsilon w_1(t_f)+\varepsilon^2 w_2(t_f)+\mathrm{O}(\varepsilon^3) = \psi_f = 0
$$

Using the above in (14), (15), and (17) we obtain

$$
\begin{aligned}
a_1 &= \frac{-\psi_0}{t_f} && (21)\\
a_2 &= \psi_0 && (22)\\
a_4 &= \frac{t_f^2}{\psi_0^2}\cos(\psi_0) && (23)\\
a_3 &= \frac{1}{t_f}\left(\frac{1}{a_1^2} - a_4\right) && (24)\\
a_6 &= \frac{1}{8a_1^4}\sin(2a_2) - \frac{2a_3}{a_1^3}\cos(a_2) + -\frac{a_4}{a_1^2}\sin(a_2) && (25)\\
a_5 &= \frac{1}{t_f}\left(-a_6 - \frac{2a_3}{a_1^3}\right) && (26)
\end{aligned}
$$

The three term approximation in (11) together with the constants defined above ensure that the boundary conditions are satisfied for *any* λ_2 and V.

Approximating $y(t)$: We next consider the $\dot{y}$ equation in (4). In the following, we shall approximate the solution for which both $\psi(t_f) = \psi_f$ and $y(t_f) = y_f$ while ignoring the boundary condition on $x(t_f)$. Expanding ψ about the $\mathrm{O}(1)$ approximation and then integrating yields

$$
y(t) = V\int_{t_0}^{t}\left(\sin(w_0) + \cos(w_0)\left(\varepsilon w_1 + \varepsilon^2 w_2\right) - \sin(w_0)\frac{\varepsilon^2 w_1^2}{2} + \mathrm{O}(\varepsilon^3)\right)dt \tag{27}
$$

Define

$$
\begin{aligned}
I_1(t) &= \int \sin(w_0)dt && (28)\\
I_2(t) &= \int w_1\cos(w_0)dt && (29)\\
I_{3_a}(t) &= \int w_2\cos(w_0)dt && (30)\\
I_{3_b}(t) &= \int w_1^2\sin(w_0)dt && (31)\\
I_3(t) &= I_{3_a}(t) - \frac{1}{2}I_{3_b}(t) && (32)
\end{aligned}
$$

It follows that

$$
y(t) = V\left(I_1(t) - I_1(t_0)\right) + \varepsilon V\left(I_2(t) - I_2(t_0)\right) + \varepsilon^2 V\left(I_3(t) - I_3(t_0)\right) + y_0 \tag{33}
$$

Expressions for $I_1(t)$, $I_2(t)$, and $I_3(t)$ are obtained using (16):

$$
\begin{aligned}
I_1(t) &= f_0 && (34)\\
I_2(t) &= -\frac{1}{a_1^2}f_3 + a_3 f_4 + a_4 f_1 && (35)\\
I_{3_a}(t) &= -\frac{1}{8a_1^4}f_{15} + \frac{a_3}{a_1^2}f_{16} + 2\frac{a_3}{a_1^3}f_3 + \frac{a_4}{a_1^2}f_2 + a_5 f_4 + a_6 f_1 && (36)\\
I_{3_b}(t) &= -\frac{f_{14}}{a_1^4} - \frac{2}{a_1^2}\left(a_2 f_{16} + a_4 f_2\right) + a_3^2 f_{17} + 2a_3 a_4 f_6 + a_4^2 f_0 && (37)
\end{aligned}
$$

We further define

$$
\begin{aligned}
p_0 &= y_f - y_0\\
p_1 &= I_1(t_f) - I_1(t_0)\\
p_2 &= I_2(t_f) - I_2(t_0)\\
p_3 &= I_3(t_f) - I_3(t_0) && (38)
\end{aligned}
$$

At the final time, we have

$$F_y(\lambda_2^{(y)},V) = \lambda_2^{(y)^2}V^3q_3 + \lambda_2^{(y)^2}V^2p_2 + \lambda_2^{(y)^2}Vp_1 - p_0 = 0 \tag{39}$$

where we have used $\varepsilon = \lambda_2^{(y)}V$. We have replaced λ_2 by $\lambda_2^{(y)}$ to indicate that setting $\lambda_2 = \lambda_2^{(y)}$ as defined in (39) guarantees that $y(t_f) = y_f$.

We solve for $\lambda_2^{(y)}$:

$$\lambda_2^{(y)} = \frac{\sqrt{V}p_2 \pm \sqrt{V(p_2^2 - 4p_3p_1) + 4p_3p_0}}{2V^{3/2}p_3} \tag{40}$$

Approximating $x(t)$: We next consider the $\dot{x}$ equation in (4). Expanding ψ about the O(1) approximation and then integrating yields

$$\begin{aligned} x(t) &= V\int_{t_0}^{t}\left(\cos(w_0) - \sin(w_0)\left(\varepsilon w_1 + \varepsilon^2 w_2\right) - \cos(w_0)\frac{\varepsilon^2 w_1^2}{2}\right)dt + \mathrm{O}(\varepsilon^3) \\ &\approx V\left(K_1(t) - K_1(t_0) - \varepsilon\left(K_2(t) - K_2(t_0)\right) - \varepsilon^2\left(K_3(t) - K_3(t_0)\right)\right) + x_0 \end{aligned} \tag{41}$$

where

$$K_1(t) = \int \cos(w_0(t))dt = f_1(t) \tag{42}$$

$$\begin{aligned} K_2(t) &= \int w_1(t)\sin(w_0(t))dt \\ &= \int\left[-\frac{1}{a_1^2}\cos(w_0(t)) + a_3t + a_4\right]\sin(w_0(t))dt \\ &= -\frac{1}{a_1^2}f_2(t) + a_3f_6(t) + a_4f_0(t) \end{aligned} \tag{43}$$

$$K_3(t) = K_{3_a}(t) + \frac{1}{2}K_{3_b}(t) \tag{44}$$

$K_{3_a}(t)$ is given by:

$$\begin{aligned} K_{3_a}(t) &= \int w_2(t)\sin(w_0(t))dt \\ &= \int\left[-\frac{1}{8a_1^4}\sin(2w_0(t)) + \frac{a_3}{a_1^2}t\sin(w_0(t)) + 2\frac{a_3}{a_1^3}\cos(w_0(t)) + \frac{a_4}{a_1^2}\sin(w_0(t))\right. \\ &\quad \left. + a_5t + a_6\right]\sin(w_0(t))dt \\ &= -\frac{1}{8a_1^4}f_8(t) + \frac{a_3}{a_1^2}f_9(t) + 2\frac{a_3}{a_1^3}f_2(t) + \frac{a_4}{a_1^2}f_5(t) + a_5f_6(t) + a_6f_0(t) \end{aligned} \tag{45}$$

$K_{3_b}(t)$ is given by:

$$\begin{aligned} K_{3_b}(t) &= \int w_1^2(t)\cos(w_0(t))dt \\ &= \int\left(\frac{1}{a_1^4}\cos^2(w_0(t))dt - 2\frac{r}{a_1^2}\cos(w_0(t)) + r^2\right)\cos(w_0(t))dt \end{aligned} \tag{46}$$

Note that:

$$\int \cos^3(w_0(t))dt = f_{11}(t) \tag{47}$$

$$\begin{aligned} \int r\cos^2(w_0(t))dt &= \int(a_3t + a_4)\cos^2(w_0(t))dt \\ &= a_3f_{12}(t) + a_4f_3(t) \end{aligned} \tag{48}$$

$$\begin{aligned}\int r^2\cos(w_0(t))dt &= \int \left(a_3^2t^2\cos(w_0(t))dt + 2a_3a_4t\cos(w_0(t))dt + a_4^2\cos(w_0(t))\right)dt \\ &= a_3^2 f_{13}(t) + 2a_3a_4 f_4(t) + a_4^2 f_1(t) \end{aligned} \quad (49)$$

Substituting (47-49) into (46), we obtain

$$K_{3_b}(t) = \frac{1}{a_1^4} f_{11}(t) - \frac{2}{a_1^2}\left(a_3 f_{12}(t) + a_4 f_3(t)\right) + a_3^2 f_{13}(t) + 2a_3a_4 f_4(t) + a_4^2 f_1(t) \quad (50)$$

At the final time, the x-position is found by using (41) with $t = t_f$:

$$x(t_f) = V\left(K_1(t_f) - K_1(t_0) - \varepsilon\left(K_2(t_f) - K_2(t_0)\right) - \varepsilon^2\left(K_3(t_f) - K_3(t_0)\right)\right) + x_0 \quad (51)$$

Defining

$$\begin{aligned} q_0 &= y_f - y_0 \\ q_1 &= K_1(t_f) - K_1(t_0) \\ q_2 &= K_2(t_f) - K_2(t_0) \\ q_3 &= K_3(t_f) - K_3(t_0) \end{aligned} \quad (52)$$

$$(53)$$

It follows that:

$$F_x(\lambda_2, V) = Vq_3\varepsilon^2 + q_2V\varepsilon - Vq_1 + q_0 = 0 \quad (54)$$

Computing the Control Law: Thus far, we have constructed an asymptotic approximation of the solution to (10) given by (11) that satisfies the initial and final conditions, $\psi(t_0)$ and $\psi(t_f)$, respectively, for any λ_2 and V such that $\varepsilon = \lambda_2 V$ is small in the asymptotic sense. Once λ_2 and V are determined, the control law is computed as follows. Differentiating the approximate solution at time $t = 0$ and using (9), we obtain

$$\begin{aligned} c &= \lambda_2 x_0 - \dot{\hat{\psi}}(0) \\ &= \lambda_2 x_0 - \left(\dot{w}_0(0) + \varepsilon\dot{w}_1(0) + \varepsilon^2\dot{w}_2(0)\right) \end{aligned}$$

where

$$\begin{aligned} \dot{w}_0(0) &= a_1 \\ \dot{w}_1(0) &= \frac{1}{a_1}\sin(a_2) + a_3 \\ \dot{w}_2(0) &= -\frac{1}{4a_1^3}\cos(2a_2) - \frac{a_3}{a_1^2}\sin(a_2) + \frac{a_4}{a_1}\cos(a_2) + a_5 \end{aligned}$$

Given c, the *linear* control law (9) is obtained. Hence, we only need λ_2 and V.

IV. Feasibility Regions

An approximate solution to the problem specified in Section II must simultaneously satisfy (39) and (54):

$$F_x(\lambda_2, V) = F_y(\lambda_2, V) = 0$$

If there exists a real number λ_2 and $V \in [V_{min}, V_{max}]$ that satisfies the above, the approximate trajectory guarantees that $x(t_f) = x_f$, $y(t_f) = y_f$ and $\psi(t_f) = \psi_f$. However, given a desired final time and initial aircraft position and heading, it is not clear whether a feasible pair (λ_2, V) exists. It is to be emphasized again that the motivation of the proposed approach is to enable an air-traffic controller to dynamically specify an arrival time for an aircraft that may change depending on conditions on the ground and in the air.

Our approach to this problem is as follows:

Step 1: Specify Initial and Final Data

1. Specify initial A/C data: (t_0, x_0, y_0, ψ_0)

2. Specify final A/C data: (t_f, x_f, y_f, ψ_f)
3. Specify bounds on velocity: $[V_{min}, V_{max}]$ and final x_f: $[x_{f_{min}}, x_{f_{max}}]$

Step 2: Estimate Bounds on Feasible CTA Windows

- Given an initial aircraft position and heading it may not be possible to reach a desired final position by the desired final (arrival) time. This may be due to (1) limits on the maximum and minimum velocities, (2) limits on the maximum and minimum turn rates (bank angle), and (3) there does not exist an optimal solution with respect to the cost functional.

  For example, suppose an aircraft is heading due east at $(t_0 = 0(s), x_0 = 0(nm), y_0 = 0(nm), \psi_0 = 0(rad))$ and the desired final data given by $(t_f = 150(s), x_f = 16(nm), y_0 = 0(nm), \psi_0 = 0(rad))$. Suppose further that the velocity bounds are $V_{min} = 150(kts)$ and $V_{max} = 300(kts)$. At $V = V_{max}$ and with heading angle pointed straight at the target $(\psi(t) = 0)$, the final position $x(t_f) = 300 \cdot t_f = 12.5(nm) < x_f = 16(nm)$. Hence, given the initial data, it would not be possible to achieve any arrival times less than 192 seconds. If a flight management system requires the ability to specify CTA windows, then (dynamic) bounds on $[t_{f_{min}}\ t_{f_{max}}]$ which guarantee optimality would be helpful. In Fig. 2., we show four different aircraft positions. Given the data in Step 1, feasible CTA windows are rapidly generated and shown in brackets.

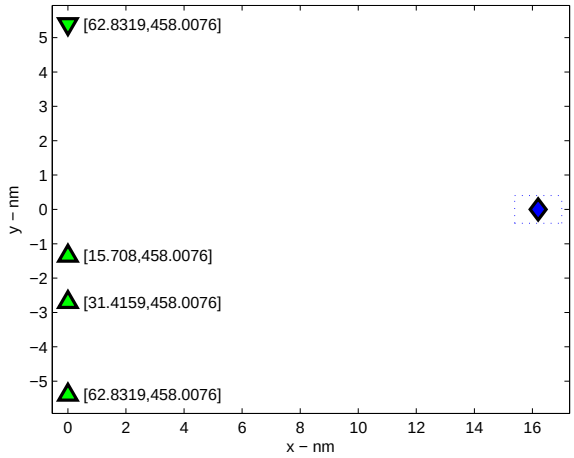

Figure 2. Time of arrival windows for four aircraft. The diamond denotes the final way point with corresponding bounds in x and y indicated by dashes. Numbers enclosed in the brackets denote the estimated minimum and maximum arrival times for which a search may be performed.

- The CTA bounds are dynamic in the sense that at every time step, the initial data changes. To elaborate further, consider a single aircraft trajectory. Define $t_0^{(opt)} \in [t_0, t_f)$ to be the time where the optimal trajectory commences. That is, the time for which an optimal u^* is applied in (4). Denote this interval as $\mathscr{T}_{opt} = [t_0^{(opt)}, t_f]$. For times $t \in [t_0, t_0^{(opt)})$, we assume the aircraft is flying a non-optimal trajectory. This could be, for example, a holding pattern or a straight flight segment. $t_0^{(opt)}$ is updated at every instant aircraft data is made available. Dynamic bounds on the CTA windows may be calculated whenever $t_0^{(opt)}$ changes.

V. Examples

Example 1 (Optimal Trajectories for a Single Aircraft) *We take as the initial conditions $x_0 = -500(m)$ and $y_0 = -500(m)$ and simulate forty equally spaced initial heading angles between -135 and $+135$ degrees. The velocity used was fixed at 800 km/hr or 431.9654 knots. The asymptotic solutions are shown in Fig. 3. Next, we leverage Broyden's method to rapidly converge to the optimal solutions. This is shown in Fig. 4.*

Example 2 (Optimal Merging of Multiple Aircraft with Time of Arrival Windows) *In this example we consider the problem of merging four aircraft. The problem is to determine, for each aircraft an optimal CTA window and velocity with a separation constraint (radius). To generate CTA windows, the algorithm in Steps 1-2 is applied. Fig.*

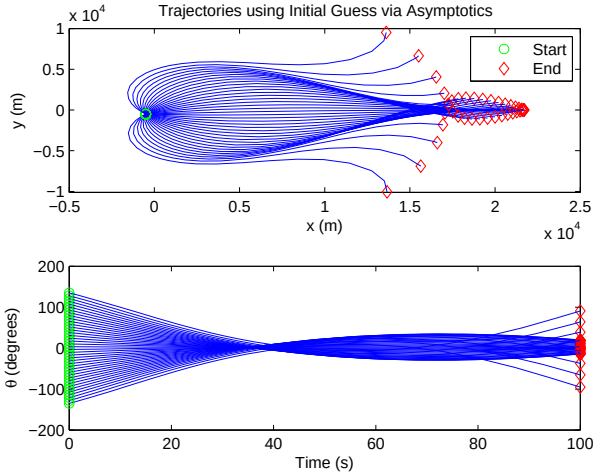

Figure 3. 40 initial heading angles between -135 and $+135$ degrees are simulated. For each simulation, parameters were obtained using the initial guess via the three-term asymptotic expansion. As the initial heading angle deviates from the final heading angle, the asymptotic solution becomes less accurate.

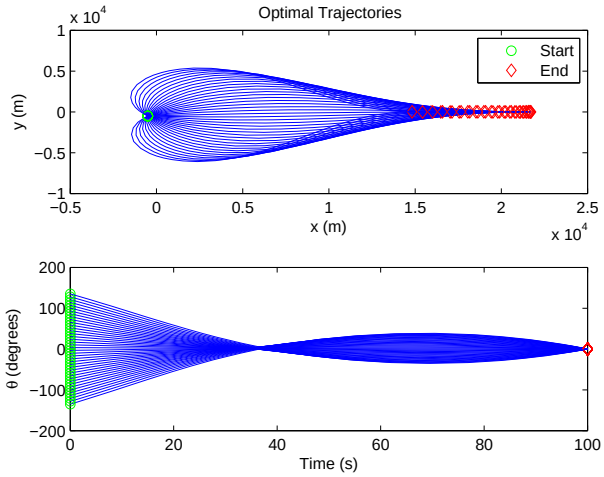

Figure 4. Optimal trajectories with 40 initial heading angles between -135 and $+135$ degrees are simulated. For each simulation, parameters were obtained via a search using Broyden's method.

5., depicts the corresponding feasible arrival time windows and velocities. A search is performed to choose CTA windows and velocities such that separation assurance constraints are satisfied. Fig. 6., depicts the resulting optimal trajectories. The separation assurance constraints are represented by dotted circles around each aircraft.

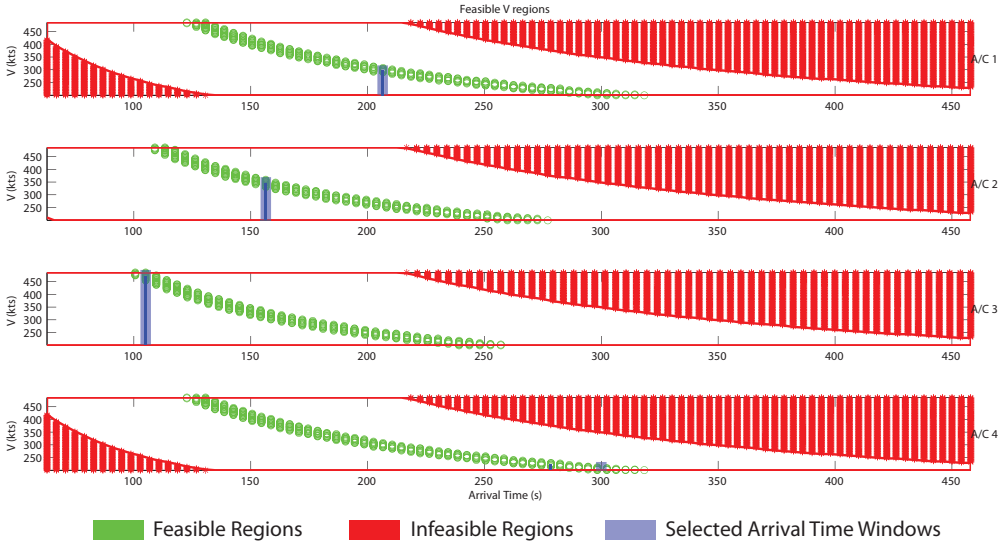

Figure 5. For each aircraft, an initial search regime $[t_{f_{min}}\ t_{f_{max}}]$ is computed. Then, time of arrival windows and corresponding velocities are computed for each aircraft. The air-traffic controller is able to select time of arrival windows for each aircraft.

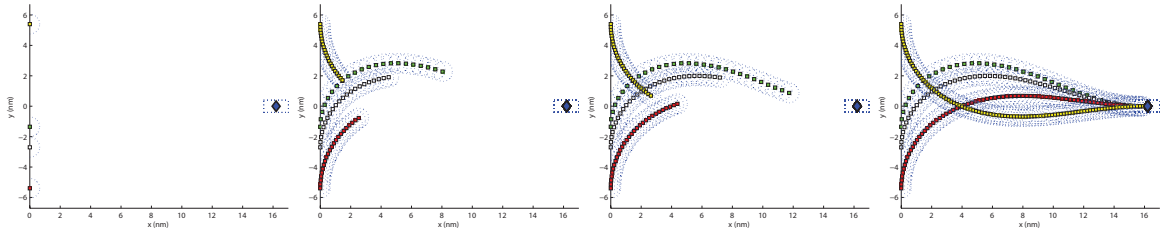

Figure 6. Optimal merging of four aircraft. Separation assurance constraints are represented by dotted circles around each aircraft. A search was performed over the feasible CTA windows and velocities shown in Fig. 5.

Example 3 (Tracking of Optimal Trajectories with an Adaptive Controller and Re-planning) *We consider the following lateral aircraft dynamics [1,2]:*

$$\begin{bmatrix} \dot{p} \\ \dot{r} \end{bmatrix} = \begin{bmatrix} f_p \\ f_r \end{bmatrix} + \begin{bmatrix} L_{\delta_a} & L_{\delta_r} \\ N_{\delta_a} & N_{\delta_r} \end{bmatrix} \begin{bmatrix} \delta_a \\ \delta_r \end{bmatrix} \tag{55}$$

and

$$\begin{bmatrix} \dot{\beta} \\ \dot{\phi} \end{bmatrix} = \begin{bmatrix} f_\beta \\ 0 \end{bmatrix} + \begin{bmatrix} \sin\alpha & -\cos\alpha \\ 1 & \tan\theta\cos\phi \end{bmatrix} \begin{bmatrix} p \\ r \end{bmatrix} \tag{56}$$

where

$$
\begin{aligned}
f_p &= \tfrac{1}{I_x(I_xI_z-I_{xz}^2)}(L_0I_yI_z+N_0I_yI_{xz}) \\
f_r &= \tfrac{1}{I_z(I_xI_z-I_{xz}^2)}(L_0I_yI_{xz}+N_0I_xI_y) \\
f_\beta &= \tfrac{\bar{q}S}{mV}(\beta C_{Y_\beta}\cos\beta+\sin\beta(C_{D_0}+\alpha C_{D_\alpha}))-\tfrac{T\cos\alpha}{mV}\sin\beta \\
&+ \tfrac{g}{V}(\sin\alpha\cos\alpha\sin\beta+\cos\alpha\sin\phi\cos\beta-\sin\alpha\cos\alpha\cos\phi\sin\beta) \\
L_{\delta_a} &= \tfrac{\bar{q}Sb}{I_x(I_xI_z-I_{xz}^2)}(I_yI_zC_{l_{\delta_a}}+I_yI_{xz}C_{n_{\delta_a}}) \\
L_{\delta_r} &= \tfrac{\bar{q}Sb}{I_z(I_xI_z-I_{xz}^2)}(I_yI_zC_{l_{\delta_r}}+I_yI_{xz}C_{n_{\delta_r}})
\end{aligned}
\tag{57}
$$

and

$$
\begin{aligned}
L_0 &= \bar{q}Sb\left[\beta C_{l_\beta}+\tfrac{b}{2V}(pC_{l_p}+rC_{l_r})\right] \\
N_0 &= \bar{q}Sb\left[\beta C_{n_\beta}+\tfrac{b}{2V}(pC_{l_p}+rC_{l_r})\right]
\end{aligned}
$$

The aerodynamic coefficients, obtained from [17], are assumed to satisfy

$$
\begin{aligned}
C_l &= C_{l_\beta}\beta+C_{l_p}p+C_{l_r}r+C_{l_{\delta\alpha}}\delta\alpha+C_{l_{\delta_r}}\delta_r \\
C_n &= C_{n_\beta}\beta+C_{n_p}p+C_{n_r}r+C_{n_{\delta\alpha}}\delta\alpha+C_{n_{\delta_r}}\delta_r \\
C_D &= C_{D_0}+C_{D_\alpha}\alpha \\
C_Y &= C_{Y_\beta}\beta
\end{aligned}
\tag{58}
$$

A description of the notation used above is provided in Table 1.

Table 1. Nomenclature: Notation description

Notation	Description	Notation	Description
θ	Pitch angle	C_D	Drag coefficient
ϕ	Roll(bank) angle	C_Y	Side force coefficient
ψ	Yaw angle	C_n	Yaw moment coefficient
α	Angle of Attack	C_l	Roll moment coefficient
β	Side slip	V	Aircraft velocity
p	Roll rate	S	Wing area
q	Pitch rate	T	Thrust force
r	Yaw rate	m	Mass of aircraft
C_L	Lift coefficient	g	Gravitational constant
$\bar{c}$	Wing aerodynamic chord	b	Wing span
x_E, y_E, h	Earth coordination values	I_x, I_y, I_z, I_{xz}	Moment of inertia w.r.t each axis

In Fig. 7, we simulate the tracking of an optimal trajectory by an adaptive backstepping controller [12,14,15,19] applied to the system dynamics given in (55-56). Stability analysis and details of its implementation are beyond the scope of this paper. Initial and final data was provided to the optimization algorithm as discussed in Section IV. In this case, proper tuning of the controller yielded accurate tracking of the optimal trajectory.

Next, we simulated failure by changing an aerodynamic coefficient in one of the aircraft models. This resulted in a deviation from the trajectory and violation of the separation assurance constraint is observed around 7.5 (s). At this time, we re-computed the optimal trajectories for all aircraft and applied the same optimization routine to determine the new CTA windows and corresponding velocities. This is shown in Fig. 8.

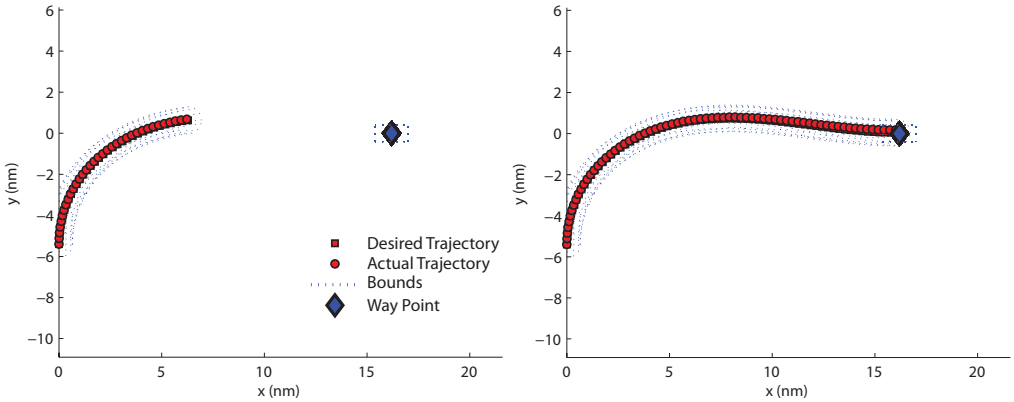

Figure 7. Tracking of Optimal Trajectory using an Adaptive Backstepping Controller.

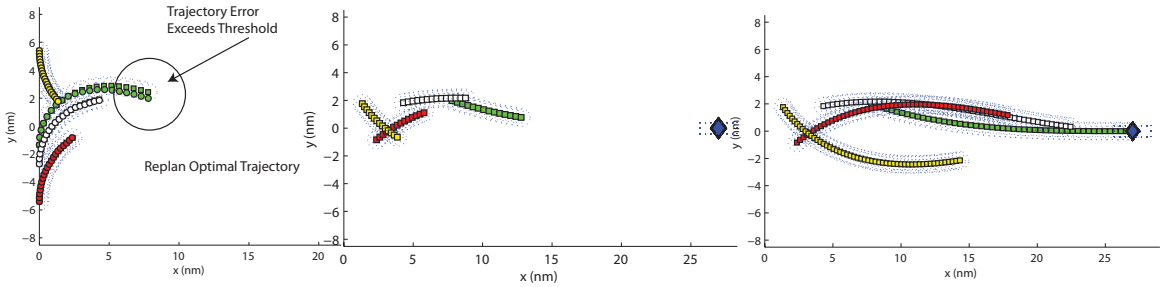

Figure 8. Tracking of Optimal Trajectory using Adaptive Backstepping Controller. Failure is simulated in one of the aircraft. This resulted in violation of the separation assurance constraint and initiated a re-optimization of the trajectories, CTA windows, and velocities of each aircraft.

VI. Conclusions

We presented a robust initialization scheme that estimates parameter values for the numerical solution of a two-point boundary value problem. The two-point boundary value problem formulation stems from the optimization of a cost functional subject to the dynamics of a simplified lateral aircraft model and other constraints. Leveraging perturbation methods, initial parameter estimates are analytically determined and used to initialize a gradient descent optimization routine which is shown to converge over a range of initial aircraft positions and heading angles. Using this approach, we were able to rapidly estimate CTA windows and corresponding aircraft velocities. Future work includes the extension of this technique to multiple waypoints with multiple CTA windows that are computed online.

References

[1]Saif A. Al-Hiddabi. Design of a flight control system for a non-minimum phase 5 dof aircraft model. In *The 11th Mediterranean Conference on Control and Automation*, pages 1–9, June 2003.

[2]Saif A. Al-Hiddabi and N. Harris McClamroch. Tracking and maneuver regulation control for nonlinear nonminimum phase systems: Application to flight control. *IEEE Transactions on Control Systems Technology*, 10(6):780–792, Nov 2002.

[3]M G Ballin, D H Williams, B D Allen, and M T Palmer. *Prototype flight management capabilities to explore temporal RNP concepts*, page 3. 2008.

[4]M. Bolender and G.L. Slater. Departure trajectory synthesis and the intercept problem. 1997.

[5]A.E. Bryson and Y.C. Ho. *Applied Optimal Control: Optimization, Estimation, and Control*. Halsted Press book'. Taylor & Francis, 1975.

[6]Metropolitan Area Demand and Operational Capacity. Capacity needs in the national airspace system and operational capacity. *Administrator*, (May), 2007.

[7]H Erzberger and H Q Lee. Optimum horizontal guidance techniques for aircraft. *Journal of Aircraft*, 8(2):95–101, 1971.

[8]L C Evans. An introduction to mathematical optimal control theory. *Lecture notes*, pages 1–126, 2009.

[9]Faa. Nextgen implementation plan 2009. *Aviation*, page 62, 2009.

[10]M.H. Holmes. *Introduction to Perturbation Methods*. Springer, 1995.

[11]Jpdo. Concept of operations for the next generation air transportation system. version 3.2. 2011.

[12]T. Lee and Y. Kim. Nonlinear adaptive flight control using backstepping and neural networks controller., journal=Journal of Guidance, Control, and Dynamics, year=2001, volume=24, pages=675682,.

[13]F.L. Lewis, D. Vrabie, and V.L. Syrmos. *Optimal Control*. John Wiley & Sons, 2012.

[14]Yi Luo, Yoo Hsiu Yeh, and Abraham K. Ishihara. Adaptive backstepping design for a longitudinal uav model utilizing a fully tuned growing radial basis function network. In *InfoTech@Aerospace 2011*, 2011.

[15]Yi Luo, Yoo Hsiu Yeh, and Abraham K. Ishihara. Robot control with a fully tuned growing radial basis function neural network. In *Internation Joint Conference on Neural Networks*, pages 342–348, San Jose, CA, Aug 2011. IEEE.

[16]Andre Michelin, Moshe Idan, and Jason L Speyer. Merging of air traffic flows. *Journal of Guidance Control and Dynamics*, 34(1):13–28, 2011.

[17]Robert C. Nelson. *Flight Stability and Automatic Control*. Mc Graw Hill, second edition, 1998.

[18]T Pecsvaradi. Optimal horizontal guidance law for aircraft in the terminal area. 1972.

[19]M. Sharma and D.G. Ward. Flight-path angle control via neuro-adaptive backstepping. *AIAA Guidance, Navigation, and Control Conference and Exhibit*,, 2002.